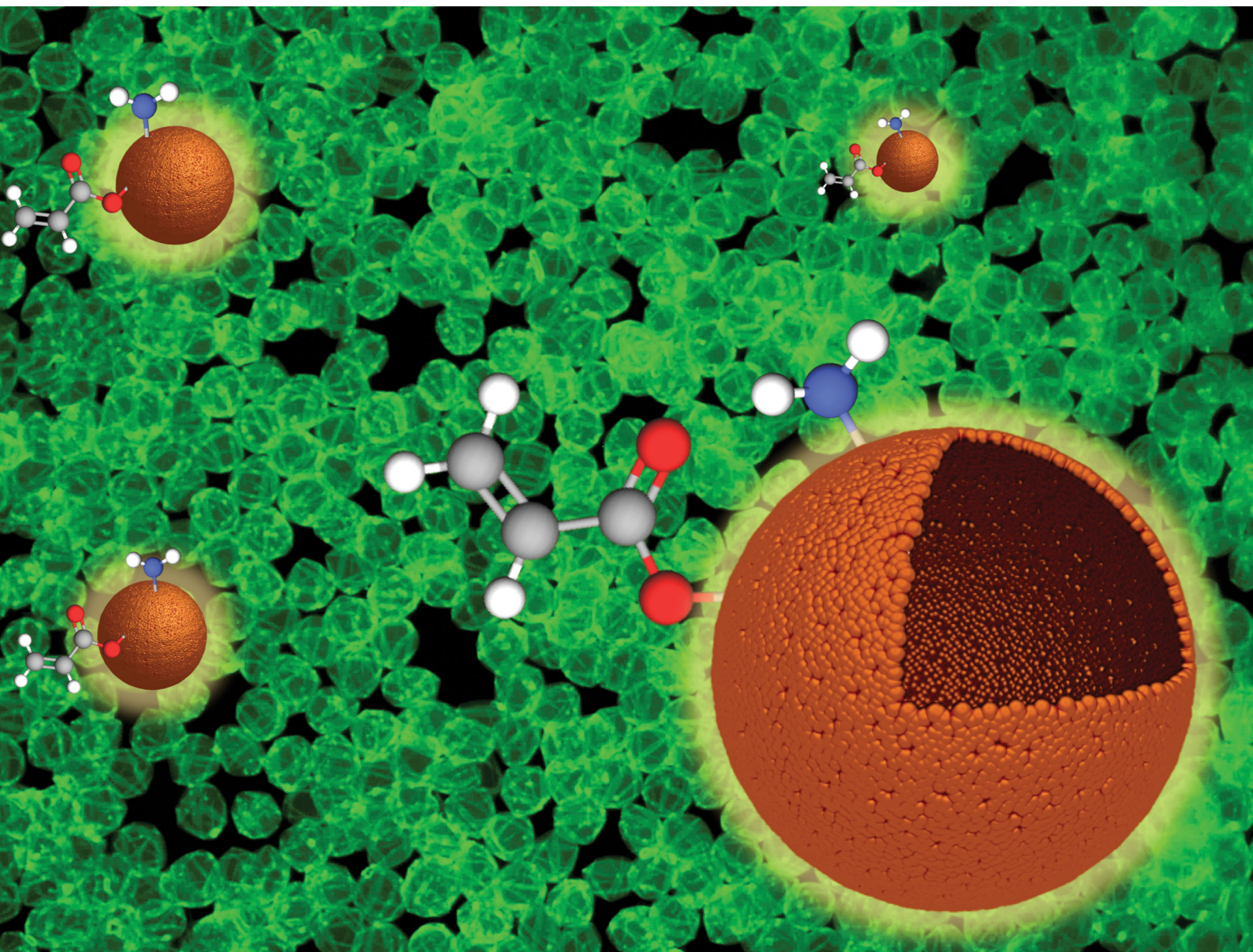


# ChemComm

Chemical Communications

rsc.li/chemcomm



ISSN 1359-7345

**COMMUNICATION**

Angana Borbora and Uttam Manna  
Synthesis of orthogonally reactive multilayered  
microcapsules



# Synthesis of orthogonally reactive multilayered microcapsules†

 Angana Borbora<sup>a</sup> and Uttam Manna  <sup>\*ab</sup>

 Cite this: *Chem. Commun.*, 2020, **56**, 7853

 Received 29th January 2020,  
 Accepted 13th March 2020

DOI: 10.1039/d0cc00618a

[rsc.li/chemcomm](http://rsc.li/chemcomm)

**In this communication, a single polymer derived multilayered microcapsule loaded with orthogonally reactive residual functional groups—acrylate and amine—is synthesized by rational association of a facile layer-by-layer (LbL) deposition process and a catalyst-free 1,4-conjugate addition reaction under ambient conditions. This approach is appropriate for controlled chemical modulations of multilayered microcapsules with various electrophiles and nucleophiles following two independent reaction pathways.**

In the past, hollow multilayered microcapsules were synthesized by sequential deposition of appropriately selected pairs of polymers and (or) polyelectrolytes on sacrificial colloidal templates.<sup>1–4</sup> Mostly, weak hydrogen-bonds, di-sulfide bonds and electrostatic interactions were used in synthesizing multilayered membranes on the colloidal templates. The selective removal of colloidal templates yielded hollow polymeric microcapsules.<sup>1–9</sup> The available empty space in the polymeric microcapsules has been utilized for confining various cargo, liquid crystals and bioactive enzymes for various relevant applications.<sup>2–4,10–13</sup> Further, the design of a single polymer derived microcapsule with the ability to tailor different desired chemical functionalities following simple chemical modifications under ambient conditions would allow to customize the micron/submicron-confined space with diverse chemical functionalities. In the past, mostly catalyst assisted ‘click’ reactions or ring-opening ‘click-type’ reactions between two distinct polymers having mutually reactive chemical moieties were introduced for developing covalently crosslinked and functional microcapsules.<sup>14–18</sup> Inspired by these results, here, a single

polymer derived orthogonally reactive hollow microcapsule is unprecedentedly synthesized for facile and controlled tailoring of chemistry with various selected nucleophiles and electrophiles, following two independent reaction pathways.

Inspired by an earlier report,<sup>19</sup> a stable and slowly growing chemically reactive polymeric nanocomplex (CRPNC) is synthesized and covalently integrated following a simple layer-by-layer (LbL) deposition process to develop an orthogonally reactive multilayered microcapsule. In the recent past, a reaction mixture of branched poly(ethyleneimine) (BPEI) and dipentaerythritol penta-acrylate (5Acl) formed a chemically reactive polymeric nanocomplex (CRPNC), which was covalently aggregated to form a shapeable gel under ambient conditions,<sup>19</sup> where amine and acrylate readily reacted through a 1,4-conjugate addition reaction and residual acrylate groups rendered the nanocomplex chemically reactive, as shown in Fig. 1A and B. Furthermore, CRPNC was integrated into different LbL constructions on planar objects to adopt different durable biomimicked and extremely liquid-repellent interfaces.<sup>20–22</sup> In the earlier reported composition (BPEI: 5Acl = 3:10) of reactants, the CRPNC that rapidly grew from 20 nm to 451 nm within 1 hour exhibited unwanted aggregation during LbL construction of CRPNC/BPEI on sacrificial templates (silica microparticles, diameter = 5 ± 0.35 μm). Thus, the reaction composition was further optimized to delay the growth of the polymeric nanocomplex during the construction of reactive multilayers on the sacrificial templates, for avoiding unwanted aggregation of the polymeric nanocomplexes. At the reaction composition of 7 (BPEI): 100 (5Acl), the growth of the polymeric nanocomplex was noted to be significantly lowered, and the size of the nanocomplex was observed to be 61 nm after 1 hour of reaction time, as shown in Fig. 1C. However, the nanocomplexes remained chemically reactive even after the change in the composition of reactants, as confirmed by attenuated total reflection-infrared spectroscopy (ATR-IR) analysis, shown in Fig. 1D, where the appearance of two characteristic IR signatures for the C–H deformation of β-carbon of the vinyl groups and the carbonyl stretching of the ester linkage at 1410 cm<sup>-1</sup> and 1735 cm<sup>-1</sup>, respectively, revealed the existence of residual acrylate

<sup>a</sup> Bio-Inspired Polymeric Materials Lab, Department of Chemistry, Indian Institute of Technology-Guwahati, Kamrup, Assam 781039, India.  
 E-mail: [umanna@iitg.ac.in](mailto:umanna@iitg.ac.in)

<sup>b</sup> Centre for Nanotechnology, Indian Institute of Technology-Guwahati, Kamrup, Assam 781039, India

† Electronic supplementary information (ESI) available: Supplementary information accounting for materials and method and Fig. S1–S6 illustrating the mono and dual chemical reactivity of the multilayered microcapsules, cross-polar microscopic image of microcapsules, topography of microcapsules and synthesis of microcapsules with smaller size of template and impact of dilution of CRPNC on microcapsule synthesis. See DOI: 10.1039/d0cc00618a



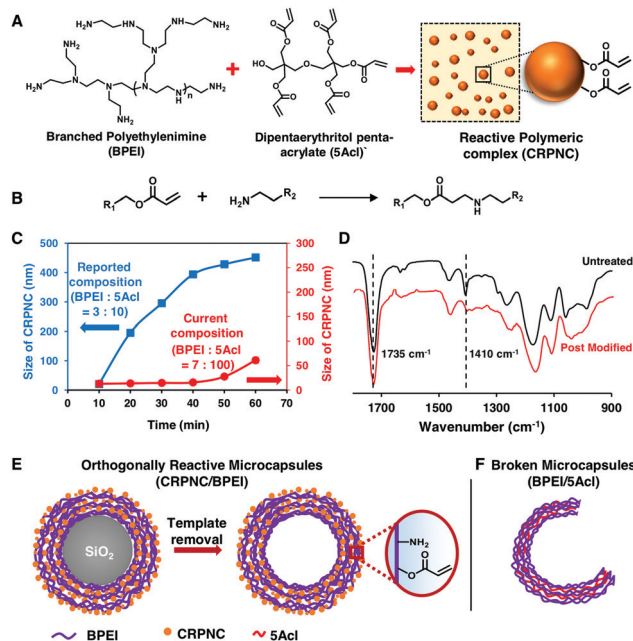


**Fig. 1** (A and B) A schematic illustration of the chemically reactive polymeric nanocomplex (CRPNC) obtained by mixing of branched poly(ethyleneimine) (BPEI) and dipentaerythritol penta-acrylate (5Acl) through 1,4-conjugate addition reaction (B). (C) Plot showing the growth of CRPNC for two distinct reaction compositions of reactants (BPEI and 5Acl). (D) ATR-IR characterization of CRPNC. (E) Schematic depiction of orthogonally reactive microcapsules of CRPNC/BPEI after dissolution of the core. (F) Illustration of broken microcapsules made of BPEI/5Acl multilayers.

groups in the polymeric nanocomplexes.<sup>19–22</sup> After the treatment of the nanocomplexes with primary amine containing small molecules (*e.g.*, 3-(dimethylamino)-1-propylamine (DMAPA)), the IR band at 1410  $cm^{-1}$  was diminished in comparison with the other IR band at 1735  $cm^{-1}$ , as shown in Fig. 1D. The 1,4-conjugate addition reaction between the amine groups of small molecules and residual acrylate groups of nanocomplexes compromised the vinyl groups selectively, and the carbonyl groups remained unaltered at the end of the formation of the covalent bond between amine and acrylate groups.

The LbL deposition of CRPNC yielded stable multilayer microcapsules, whereas the multilayers of BPEI provided broken microcapsules. The LbL integration of this slowly growing CRPNC and BPEI on a sacrificial template through 1,4-conjugate addition reaction for 5 cycles (one cycle consisted of deposition of BPEI and CRPNC sequentially; see the ESI† for more details) followed by the dissolution of the sacrificial template following hydrofluoric acid (HF) treatment (CAUTION! handle HF with appropriate safety precautions) yielded a stable hollow microcapsule (Fig. 1E).<sup>23</sup> In comparison, a multilayered (5 bilayers) membrane prepared by the sequential deposition of BPEI (polymer) and 5Acl (cross-linker) on the sacrificial colloidal template provided broken microcapsules after selective removal of the core, as shown in Fig. 1F. The successful synthesis of microcapsules was characterized by fluorescence microscopy, field emission scanning electron microscopy (FESEM), field emission transmission electron microscopy (FETEM), and atomic force microscopy (AFM) imaging, as shown in Fig. 2.

After the sequential deposition of BPEI and CRPNC on the silica microparticles (diameter =  $5 \pm 0.35 \mu m$ ), the multilayer (5 bilayers of BPEI/CRPNC) membrane coated colloidal particles were reacted with fluorescein isothiocyanate (FITC) for characterizing the polymeric coating under a fluorescence microscope, where the residual amines of BPEI polymer readily and covalently reacted with isothiocyanate groups of FITC.<sup>24</sup> A uniform coating of polymeric membrane on the colloidal particles was evident from the optical (bright field and fluorescence) microscopy images, as shown in Fig. 2A and B. After sacrificing the colloidal templates (*e.g.*, silica microparticles) following a standard HF treatment,<sup>23</sup> hollow stable microcapsules with an intact multilayered membrane of CRPNC/BPEI were obtained (Fig. 2C and D). The dilution of CRPNC can influence the formation of the microcapsule; the half-diluted solution of CRPNC provided mostly broken and distorted microcapsules (Fig. S1, ESI†) with a membrane thickness of  $22.59 \pm 2.2$  nm, whereas without dilution, a stable microcapsule with a thickness of  $40.5 \pm 3.4$  nm was obtained. In the past, multilayers of BPEI/5Acl were successfully introduced for functional coating on complex 3D (bio)silica templates.<sup>25</sup> Further, the silica microparticles that were coated with a multilayer (5 bilayers) of BPEI/5Acl yielded broken/ruptured microcapsules after dissolution of the colloidal templates, as indicated by red arrows in Fig. 2E and F. The multilayer of BPEI completely failed to sustain the osmotic pressure that was created during the core dissolution process. After air-drying,

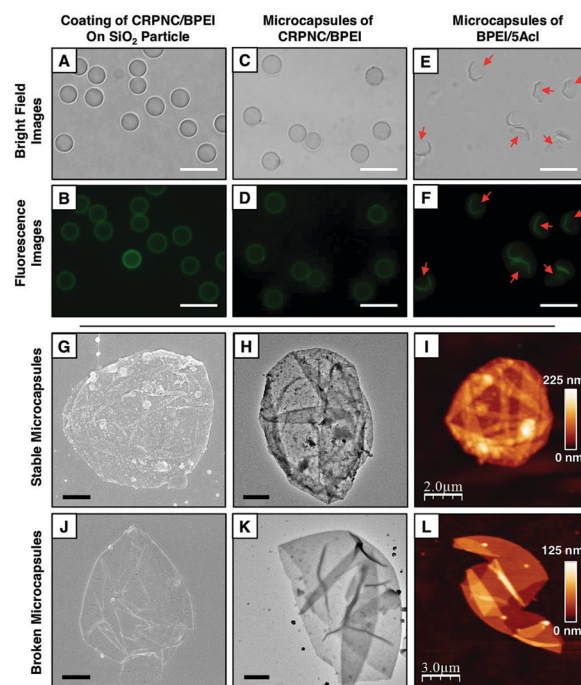


**Fig. 2** (A–F) Bright field (A, C and E) and fluorescence (B, D and F) images of coated (multilayer of CRPNC/BPEI) silica microparticles (A and B), multilayered microcapsules of CRPNC/BPEI (C and D) and BPEI/5Acl (E and F); all the multilayers were treated with fluorescein isothiocyanate (FITC) prior to imaging. Scale bar = 10  $\mu m$ . (G–L) FESEM (G and H), FETEM (I and K) and AFM (I and L) images of microcapsules made of multilayers (5 bilayers) of CRPNC/BPEI (G–I; stable capsules) and BPEI/5Acl (J–L; broken capsules). Scale bar = 1  $\mu m$  for G, H, J and K.

the hollow microcapsules collapsed with arbitrary folding of the multilayered membrane, as characterized through both FESEM and FETEM images in Fig. 2G, H, J and K. This simple demonstration further validated the successful removal of colloidal templates and existence of flexibility in the CRPNC/BPEI multilayered microcapsules. Furthermore, the FESEM images (Fig. 2G) revealed the presence of nano-features in the multilayered membrane of CRPNC. Again, an AFM image reconfirmed that the membranes of CRPNC/BPEI consists of additional nano-domains, as shown in Fig. 2I. The roughness in the microcapsules is due to the random deposition of nanocomplex, as the cross polar image in Fig. S2 (ESI<sup>†</sup>) confirmed no existence of any ordered structure in the multilayer membrane. Such added nano-features (Fig. S3, ESI<sup>†</sup>) in the empty microcapsules could be useful in developing functional interfaces.<sup>26,27</sup> However, no such appearance of nano-topography was noted for ruptured microcapsules of BPEI/5Acl, as shown in Fig. 2J–L. Even sub-micron sized capsules were successfully synthesized, as shown in Fig. S4 (ESI<sup>†</sup>).

Thereafter, the available residual reactivity of the nano-featured, flexible and hollow multilayered (5 bilayers) microcapsules of CRPNC/BPEI was characterized in detail. As expected, the multilayered microcapsule was associated with two orthogonally reactive distinct residual chemical groups—acrylate and amine. The freshly prepared polymeric microcapsules of CRPNC/BPEI were characterized with standard ATR-IR spectra, where the strong emergence of two distinct and characteristic IR signatures (black line, Fig. 3B) for (i) the C–H deformation of  $\beta$ -carbon of vinyl groups at  $1410\text{ cm}^{-1}$  and (ii) carbonyl stretching at  $1735\text{ cm}^{-1}$  unambiguously supports the presence of residual acrylate groups even in the multilayered microcapsules of CRPNC/BPEI. Further, these residual acrylate groups in microcapsules remained highly reactive towards primary amine-containing small molecules. After the treatment of the as-synthesized microcapsules with DMAPA, the residual acrylate groups in the microcapsules readily reacted with primary amines of DMAPA through 1,4-conjugate addition reaction,

as is evident from the IR spectra shown in Fig. 3B. During this reaction process, the vinyl moiety of the acrylate group was consumed and the carbonyl group remained intact. The IR signature for the carbonyl group acts as an internal reference to monitor the progress of 1,4-conjugate addition reaction between amine and acrylate. After the treatment of the as-synthesized microcapsules with DMAPA, the characteristic IR band (red line, Fig. 3B) at  $1410\text{ cm}^{-1}$  for C–H stretching of  $\beta$ -carbon of vinyl groups depleted significantly with respect to the normalized IR signature for carbonyl groups ( $1735\text{ cm}^{-1}$ ).<sup>20–22</sup> This result strongly validates the existence of chemically reactive residual acrylate groups in the multilayered microcapsules of CRPNC/BPEI. Furthermore, freshly prepared microcapsules were also separately treated with fluorescein isothiocyanate (FITC), where the isothiocyanate groups are known to react readily with primary amine groups.<sup>24</sup> After the FITC treatment of the microcapsules, the fluorescence signal was noted under a fluorescence microscope, as shown in Fig. S5B (ESI<sup>†</sup>). In a control study, the microcapsules that were pre-modified with 2-(acryloyloxy)ethyltrimethyl-ammonium chloride (AETMAC) through 1,4-conjugate addition reaction, prior to a similar treatment with FITC, appeared dark under a fluorescence microscope (Fig. S5D, ESI<sup>†</sup>). The amine groups in the microcapsules were consumed during the pre-treatment of the microcapsules with AETMAC, and eventually, the isothiocyanate moiety of FITC failed to react covalently with the AETMAC-treated microcapsule, due to the lack of availability of amine groups. However, the residual acrylate groups remained unaffected during the treatment of the freshly prepared microcapsules with FITC, as confirmed through ATR-IR analysis. Right after the treatment of microcapsules with FITC, a characteristic IR peak for the –N–C=S band appeared at  $1570\text{ cm}^{-1}$ ,<sup>28</sup> which reconfirmed the covalent immobilization of FITC on the multilayered microcapsules. However, during this chemical reaction, the residual acrylate groups remained intact, as is evident from the unaffected IR signature at  $1410\text{ cm}^{-1}$  for the C–H deformation of  $\beta$ -carbon of vinyl groups. Thus, these simple demonstrations unambiguously

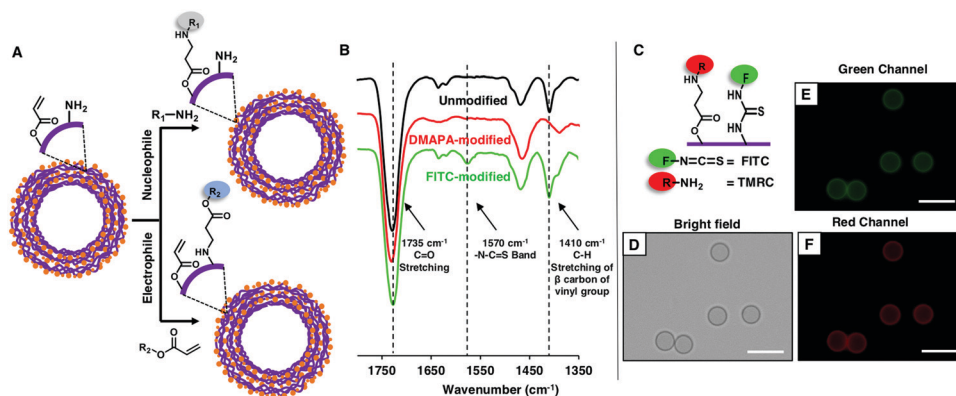


**Fig. 3** (A) Schematic representation of orthogonally reactive microcapsules loaded with residual acrylate and amine groups, where the residual acrylates and amines are capable of reacting with various nucleophiles and electrophiles, respectively. (B) ATR-IR spectra of multilayered microcapsules of CRPNC/BPEI before (black) and after post-covalent modification with DMAPA (red) and fluorescein isothiocyanate (FITC, green). (C) Schematic depiction of post-covalent modification of residual acrylate and amine with tetramethylrhodamine cadaverine (TMRC) and FITC, respectively. (D–F) Bright field (D) and fluorescence (E and F) microscopy images of multilayered microcapsules of CRPNC/BPEI after sequential post covalent modification with TMRC and FITC. Scale bar = 10  $\mu\text{m}$ .

revealed the existence of two orthogonally reactive chemical moieties in the synthesized multilayered microcapsules. Moreover, an appropriate selection of nucleophiles or electrophiles would allow to modify the synthesized microcapsules following two independent chemical reactions, as shown in Fig. 3A. Further experiments were designed to illustrate the orthogonal reactivity of the two distinct residual chemistries (*i.e.*, acrylate and amine) in the synthesized multilayered microcapsules of CRPNC/BPEI. Freshly prepared microcapsules were sequentially exposed to tetramethylrhodamine cadaverine (TMRC) and FITC, prior to examining under a fluorescence microscope, where the primary amine of TMRC and isothiocyanate of FITC readily and covalently reacted with both the residual acrylate and amine of multilayered microcapsules, respectively. The appearance of characteristic fluorescence signals for both FITC (Fig. 3E) and TMRC (Fig. 3F) validated the post covalent modification of microcapsules with both TMRC and FITC. However, microcapsules that were modified with either DMAPA or AETMAC, prior to similar and sequential exposure to TMRC and FITC, behaved differently. The DMAPA-treated microcapsule was capable of reacting only with FITC (Fig. S6B and C, ESI<sup>†</sup>), whereas the AETMAC-treated microcapsule covalently reacted only with TMRC (Fig. S6E and F, ESI<sup>†</sup>). Furthermore, the microcapsules that were pre-treated with both DMAPA and AETMAC and exposed sequentially to both FITC and TMRC failed to react with both FITC and TMRC. As expected, the fluorescence signals for any of these fluorophores were not observed from the microcapsules under the microscope (Fig. S6H and I, ESI<sup>†</sup>). Furthermore, such a chemical approach has the ability for optimizing desired and diverse chemical functionality even at the exterior and interior of the multilayered membrane of hollow microcapsules during the synthesis of multilayered coatings of chemically reactive polymeric nano-complexes (CRPNCs).

In conclusion, in this current study, an orthogonally reactive multilayered and nano-featured microcapsule was synthesized following a LbL deposition of CRPNC through 1,4-conjugate addition reaction under ambient conditions. Two distinct residual and chemically reactive groups provided a facile basis for tailoring the chemistry of multilayered microcapsules with various nucleophiles (*e.g.* alkylamines, thiols, *etc.*) and electrophiles (*e.g.* thioesters, acrylates, acid chlorides, *etc.*) following two independent chemical reactions. Such single polymer derived, chemically reactive and covalently crosslinked microcapsules having additional nano-topography on the polymeric membrane have immense potential in various applied and fundamental studies. This simple chemical approach could be extended for applications related to targeted drug delivery,<sup>7</sup> catalysis,<sup>8</sup> chemical sensing<sup>12</sup> and biomimicked wettability<sup>26</sup> in the near future.

We acknowledge the financial support from the Department of Board of Research in Nuclear Sciences (BRNS) (34/20/31/2016-BRNS,

DAE-YSRA) and Ministry of Electronics and Information Technology (grant no. 5(9)/2012-NANO). We thank the Central Instrument Facility (CIF) and the Department of Chemistry, Indian Institute of Technology-Guwahati for their generous assistance in executing various experiments and for the infrastructure. A. B. thanks the Council of Scientific & Industrial Research (CSIR, India) for the doctoral fellowship.

## Conflicts of interest

There are no conflicts to declare.

## Notes and references

- 1 E. Donath, G. B. Sukhorukov, F. Caruso, S. A. Davis and H. Möhwald, *Angew. Chem., Int. Ed.*, 1998, **37**, 2202.
- 2 C. S. Peyratout and L. Dähne, *Angew. Chem., Int. Ed.*, 2004, **43**, 3762.
- 3 W. Tong, X. Song and C. Gao, *Chem. Soc. Rev.*, 2012, **41**, 6103.
- 4 R. Kurapati, T. W. Groth and A. M. Raichur, *ACS Appl. Bio Mater.*, 2019, **2**, 5512.
- 5 O. Shchepelina, I. Drachuk, M. K. Gupta, J. Lin and V. V. Tsukruk, *Adv. Mater.*, 2011, **23**, 4655.
- 6 Y.-T. Huang, H. Zhang, X.-J. Wan, D.-Z. Chen, X.-F. Chen, X. Ye, X. Ouyang, S.-Y. Qin, H.-X. Wen and J.-N. Tang, *J. Mater. Chem. A*, 2017, **5**, 7482.
- 7 W. Xu, P. A. Ledin, Z. Iatridi, C. Tsitsilianis and V. V. Tsukruk, *Angew. Chem., Int. Ed.*, 2016, **55**, 4908.
- 8 R. Chandrawati, L. H. Rigau, D. Vanderstraaten, S. A. Lokuliyana, B. Stadler, F. Albericio and F. Caruso, *ACS Nano*, 2010, **4**, 1351.
- 9 Z. Feng, Z. Wang, C. Gao and J. Shen, *Chem. Mater.*, 2007, **19**, 4648.
- 10 W. Tong and C. Gao, *J. Mater. Chem.*, 2008, **18**, 3799.
- 11 X. Guo, K. S. Gonzalez and D. M. Lynn, *Chem. Mater.*, 2019, **31**, 7443.
- 12 J. K. Gupta, S. Sivakumar, F. Caruso and N. L. Abbott, *Angew. Chem., Int. Ed.*, 2009, **48**, 1652.
- 13 P. Shi, J. Qin, X. Wu, L. Wang, T. Zhang, D. Yang, X. Zan and D. Appelhans, *ACS Appl. Mater. Interfaces*, 2019, **11**, 39209.
- 14 G. K. Such, E. Tjipto, A. Postma, A. P. R. Johnston and F. Caruso, *Nano Lett.*, 2007, **7**, 1706.
- 15 F. Cavalieri, A. Postma, L. Lee and F. Caruso, *ACS Nano*, 2009, **3**, 234.
- 16 C.-J. Huang and F.-C. Chang, *Macromolecules*, 2009, **42**, 5155.
- 17 E. M. Saurer, R. M. Flessner, M. E. Buck and D. M. Lynn, *J. Mater. Chem.*, 2011, **21**, 1736.
- 18 X. Guo, M. C. D. Carter, V. Appadoo and D. M. Lynn, *Biomacromolecules*, 2019, **20**, 3464.
- 19 A. M. Rather and U. Manna, *Chem. Mater.*, 2016, **28**, 8689.
- 20 D. Parbat and U. Manna, *Chem. Sci.*, 2017, **8**, 6092.
- 21 A. Das, S. Sengupta, J. Deka, A. M. Rather, K. Raidongia and U. Manna, *J. Mater. Chem. A*, 2018, **6**, 15993.
- 22 D. Parbat, A. Das, K. Maji and U. Manna, *J. Mater. Chem. A*, 2020, **8**, 97.
- 23 Y. Zhang, Y. Guan, S. Yang, J. Xu and C. C. Han, *Adv. Mater.*, 2003, **15**, 832.
- 24 O. Konievab and A. Wagner, *Chem. Soc. Rev.*, 2015, **44**, 5495.
- 25 G. Wang, Y. Fang, P. Kim, A. Hayek, M. R. Weatherspoon, J. W. Perry, K. H. Sandhage, S. R. Marder and S. C. Jones, *Adv. Funct. Mater.*, 2009, **19**, 2768.
- 26 G. Wu, J. An, X.-Z. Tang, Y. Xiang and J. Yang, *Adv. Funct. Mater.*, 2014, **24**, 6751.
- 27 K. Chen, S. Zhou, S. Yang and L. Wu, *Adv. Funct. Mater.*, 2015, **25**, 1035.
- 28 C. N. R. Rao and R. Venkataraghavan, *Spectrochim. Acta*, 1962, **18**, 541.